

**The Effects of High Temperature Gas Nitriding on Mechanical and Physical Properties
of Austenitic Stainless Steel**

by

Mohd Shafizan bin Muda

Dissertation submitted in partial fulfilment of

the requirements for the

Bachelor of Engineering (Hons)

(Mechanical Engineering)

JANUARY 2009

Universiti Teknologi PETRONAS

Bandar Seri Iskandar

31750 Tronoh

Perak Darul Ridzuan

CERTIFICATION OF APPROVAL

**The Effects of High Temperature Gas Nitriding on Mechanical and Physical Properties
of Austenitic Stainless Steel**

by

Mohd Shafizan Bin Muda

A project dissertation submitted to the
Mechanical Engineering Programme
Universiti Teknologi PETRONAS
in partial fulfilment of the requirement for the
BACHELOR OF ENGINEERING (Hons)
(MECHANICAL ENGINEERING)

Approved by,

(Assoc. Prof Dr. Patthi Hussain)

UNIVERSITI TEKNOLOGI PETRONAS

TRONOH, PERAK

January 2009

CERTIFICATION OF ORIGINALITY

This is to certify that I am responsible for the work submitted in this project, that the original work is my own except as specified in the references and acknowledgements, and that the original work contained herein have not been undertaken or done by unspecified sources or persons.

MOHD SHAFIZAN BIN MUDA

ABSTRACT

High nitrogen stainless steels are being considered a new promising class of engineering materials. Theoretically, gas nitriding had improved fatigue life, strength and wear and localized corrosion resistance. In this work, this project is to study the effect of high temperature gas nitriding on the Austenitic Stainless Steel in term of mechanical properties and physical properties such as hardness, tensile strength and microstructure observation. The period of diffusion will be 1 hour, 5 hours and 9 hours respectively. The temperature will be constant in each experiment which is 1200°C. The samples are heated at 1200°C in a tube furnace through which nitrogen gas is allowed to pass. The nitrogen reacts with the steel penetrating the surface to form nitrides. After that, a further study was conducted to study the microstructure, tensile test and hardness before and after the nitriding experiment. The Hardness of the materials was determined using Vickers Hardness with 300g load. The microstructures were examined by means of optical microscopy. The effect of the diffusion time of nitrogen into the stainless steels sample was observed. By increasing the nitrogen diffusion, significantly improve the hardness and tensile strength.

ACKNOWLEDGEMENTS

The author wishes to take the opportunity to express his utmost gratitude to the individual that have taken the time and effort to assist the author in completing the project. Without the cooperation of these individuals, no doubt the author would have faced some minor complications through out the course.

First and foremost the author's utmost gratitude goes to the author's supervisor, Assoc. Prof Dr. Pathi Hussain. Without his guidance and patience, the author would not be succeeded to complete the project. To the Final Year Project Coordinator, Prof Dr. Vijay R Raghavan and Assoc. Prof. Dr Puteri Sri Melor Bte Megat Yussoff for provide him with all the initial information required to begin the project.

In addition, for the technicians and post graduate student in Mechanical Engineering Department, thank you for assisting the author in completing his project. To all individuals that has helped the author in any way, but whose name is not mentioned here, the author thankful for the effort and appreciate it.

TABLE OF CONTENTS

ABSTRACT		i
ACKNOWLEDGEMENTS.		ii
CHAPTER 1:	INTRODUCTION	1
	1.1 Background of Study	1
	1.2 Problem Statement	2
	1.3 Objectives and Scope of Study	3
CHAPTER 2:	LITERATURE REVIEW	4
	2.1 Improvement of the cavitation erosion resistance of an AISI 304L Austenitic Stainless Steel by high temperature gas nitriding.	4
	2.2 Effect of partial solution nitriding on mechanical properties and corrosion resistance in a type 316L austenitic stainless steel plate.	7
	2.3 Improvement of the slurry erosion resistance of an austenitic stainless steel with combinations of surface treatments: Nitriding and TiN coating.	12
CHAPTER 3:	METHODOLOGY	17
	3.1 Nitriding Experiment.	17
	3.2 Metallographic	18
	3.3 Vicker Hardness Testing.	22
	3.4 Tensile test	23
CHAPTER 4:	RESULT AND DISCUSSION	25
	4.1 Metallographic Result	25
	4.2 Vicker Hardness Testing	26
	4.3 Tensile Test	27
CHAPTER 5:	CONCLUSION.	30
REFERENCES		31

LIST OF FIGURES

FIGURE 1	Face centered cubic unit cell	1
FIGURE 2	Schematic illustrations of chromium carbide particles that have precipitated along grain boundaries in stainless steel, and the attendant zones of chromium depletion.	3
FIGURE 3	Surface at initial stages of CE for: (a and b) solution treated samples tested in CE after 5.4 ks, (c and d) samples with 0.33N (wt. %) at surface tested in CE after 14.4 ks and (e and f) samples with 0.48N (wt. %) at surface tested in CE after 14.4 ks. [4].	5
FIGURE 4	Hardness as a function of Nitrogen content [4].	6
FIGURE 5	Optical micrographs of the nitrogen-free 316L austenitic steel (a) and solution-nitrided 316L ones (b–d). The solution nitriding was carried (b) out at 1473 K–0.1MPa for (b) 0.6 ks, (c) 4.8 ks, and (d) 36 ks.[5].	9
FIGURE 6	Vickers hardness profiles of the 316L steel solution-nitrided for 0.6, 1.8, 4.8, and 36ks. [5].	9
FIGURE 7	Nominal stress-strain curves obtained by tensile for the steel A, N-0.6, N-1.8, and N-4.8. The solution-nitrided steels have much higher yield strength the nitrogen-free steel A.[5]	11
FIGURE 8	Changes in the yield strength and tensile strength as a function of solution Nitriding time in the solution-nitrided 316L steels (the value of yield strength and tensile strength were obtained by the stress–strain curves of Fig. 6).[5]	11
FIGURE 9	SEM micrographs of the fracture surfaces of plate specimens after tensile testing in (a) nitrogen-free 316L steel and (b) solution-nitrided steel (Steel N-4.8).[5]	12
FIGURE 10	Morphology of Sic particles used in slurry test.[12]	15
FIGURE 11	Accumulated erosion as a function of exposure time.[12]	16
FIGURE 12	SEM of the surface of the samples after 5 seconds testing: a) Solubilized, b) Solubilized+TiN, c) HTGN, d) HTGN+TiN, e) Expanded austenite and f) Expanded austenite + TiN.[12]	17
FIGURE 13	Sample Arrangements in the Alumina Boat	19
FIGURE 14	Sample was pushed into the tube furnace	19
FIGURE 15	Abrasive Cutters	21
FIGURE 16	316L Stainless Steel sample.	21
FIGURE 17	Hot Mounting	22
FIGURE 18	Simplimet Auto Mounting Press	22
FIGURE 19	METASERV 1000 grinder and polisher machine	23
FIGURE 20	Indentation process by using Vicker Hardness	25
FIGURE 21	UTM 100KN	26
FIGURE 22	Schematic drawing for metal rod	26
FIGURE 23	Microstructure of (a) Normalizing sample(5x) ,(b) 1hour(5x) ,(c) 5 hours (5x),(d) 9 hours Nitrogen diffusion at 1200°C of 316SS.	27
FIGURE 24	Hardness value of as received sample, 1 hour, 5 hours and 9 hours diffusion of Nitrogen	

	into Austenitic Stainless Steel	28
FIGURE 25	Stress Strain curve for normalizing, 1 hour, 5 hours, 9 hours of Nitrogen diffusion on austenitic Stainless Steel	30
FIGURE 26	Necking portion of the testing sample	30

LIST OF TABLES

Table 1	Hardness, elastic modulus and $H_{SiC}/H_{Surface}$ ratios of the studied samples[12] .	15
Table 2	Erosion rates of the specimens. [12]	16
Table 3	Standard dimension for tensile test E8M	26
Table 4	Summary of stress strain curve	31

CHAPTER 1

INTRODUCTION

1.1 Background of Study

Stainless steels may be defined as complex alloy steels containing a minimum of 10.5% Cr with or without other elements to produce austenitic, ferritic, duplex (ferritic-austenitic), martensitic, and precipitation-hardening grades. AISI uses a three-digit code for stainless steels[1]. Austenitic stainless steels constitute about 65-70% of the total stainless steel production in United States and have occupied a dominant position because of their corrosion resistance such as strength and toughness at both elevated and ambient temperature, excellent cryogenic properties, esthetic appeal, and varying specific combination and properties that can be obtained by different compositions within the group of steel. Austenitic stainless steels have an austenitic, face centered cubic (fcc) crystal structure (see figure 1). Austenite is formed through the generous use of austenitizing elements such as nickel, manganese, and nitrogen. Chromium content typically is in the range of 16 to 26%; nickel content is commonly less than 35%

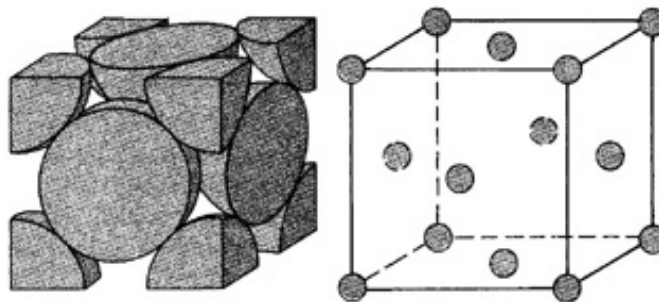


Figure 1 : Face centered cubic unit cell.[1]

1.2 Problem Statement

Austenitic stainless steels are effectively nonmagnetic in the annealed condition and can be hardened only by cold working. It is limited to certain size and shape of the metal. Some ferromagnetism may be noticed due to cold working or welding. They typically have reasonable cryogenic and high temperature strength properties. Alloying Austenitic Stainless Steel with carbon is one way of upgrading to the proper material. Any metallic element added during the making of steel for the purpose of increasing corrosion resistance, hardness, or strength. The metals used most commonly as alloying elements in stainless steel include chromium, nickel, and molybdenum [2]. The amount of carbon required in the finished steel limits the type of steel that can be made. As the carbon content of rimmed steels increase, surface quality deteriorates. Killed steels in the approximate range of 0.15 – 0.30%C may poorer surface quality and require special processing to attain surface quality comparable to steels with higher or lower carbon contents. carbon has a moderate tendency for macrosegregation during solidification, and it is often more signification than that of any alloying elements. As the carbon content in steel increases, strength increases, but ductility and weldability decrease. The addition of alloying element which is carbon will lead to chromium depletion during cooling down from above 900°C to room temperature [7]. This type of corrosion is especially prevalent in some stainless steels. When heated to temperatures between 500 and 800°C (950 and 1450°F) for sufficiently long time periods, these alloys become sensitized to intergranular attack. It is believed that this heat treatment permits the formation to small percipitate particles of chromium carbide (Cr_{23}C_6) by reaction between the chromium and carbon in the stainless steel. These particles form along the grain boundaries, as illustrated in figure 2. Both the chromium and carbon must diffuse to the grain boundaries to form the percipitates, which leaves a chromium depleted zone adjacent to the grain boundary. Consequently, this grain boundary region is vulnerable to corrosion.

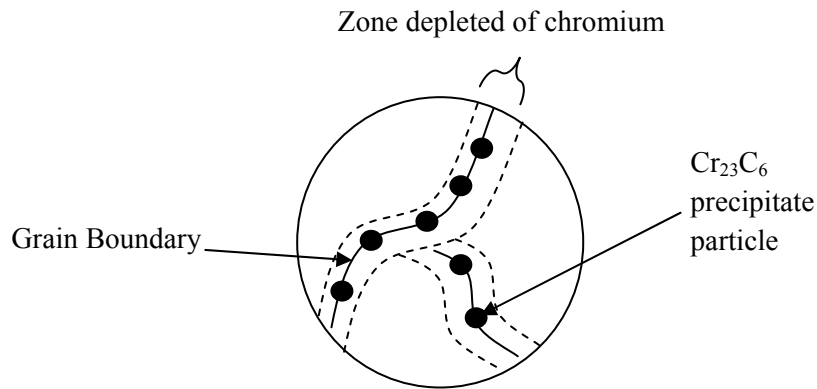


Figure 2: Schematic illustration of chromium carbide particles that have precipitated along grain boundaries in stainless steel, and the attendant zones of chromium depletion. [7]

1.3 Objectives and scope of study

The objectives of this study are to investigate and identify the change in mechanical and physical properties of Austenitic Stainless Steel by using gas nitriding at higher temperature of $1000^{\circ}\text{C} - 1200^{\circ}\text{C}$ and to compare the result with the raw Austenitic Stainless Steel.

In order to achieve this objective, a few task and research has been planned by collecting all technical and specification details regarding material background. The scope of the work is to perform nitriding at different period of nitrogen diffusion. Physical and mechanical properties were examined using hardness test, tensile test and metallography.

CHAPTER 2

LITERATURE REVIEW

There are several literatures found related to author's project about the high temperature gas nitriding. A few of the examples are regarding the improvement of the cavitations erosion resistance of an AISI 304L Austenitic Stainless Steel by high temperature gas nitriding, effect of partial solution nitriding on mechanical properties and corrosion resistance in a type 316L austenitic stainless steel plate.

2.1 Improvement of the cavitations erosion resistance of an AISI 304L Austenitic Stainless Steel by high temperature gas nitriding

Previous work show that by increasing nitrogen content, through high temperature gas nitriding, will improve the cavitation erosion resistance of an AISI 304L austenitic stainless steel[4]. From his experiment, an AISI 304L austenitic stainless steel was high temperature gas nitrided in N₂+Ar atmospheres under N₂ partial pressures up to 0.10MPa at 1423K for 21.6 ks. Nitrogen contents at the surface up to 0.48 wt. % and case depths up to 1mm were obtained. All the samples showed fully austenitic microstructures free of precipitates. Solution treated AISI 304L as well as nitrided samples were tested in distilled water in vibratory cavitation erosion (CE) equipment. Characterization of the test specimens was made by optical microscopy, electron back scattering diffraction coupled to a scanning electron microscope (EBSD–SEM), X-ray diffraction (XRD), wavelength dispersive spectroscopy (WDS) microanalysis and depth-

sensing indentation tests. All the samples had almost the same mean grain diameter, $80\mu\text{m}$, similar mesotexture and microtexture, though the nitrogen contents differed. The nitrided samples exhibited much better cavitation erosion resistance and the erosion rate was reduced by almost 8.5 times. Increasing N_2 partial pressure increased the nitrogen content at the surface, leading to an increase in the incubation period for damage and a decrease in the erosion rate. Figure 3 below shows the appearance of the surface at the initial stages of CE tests for solution treated and for nitrided samples.

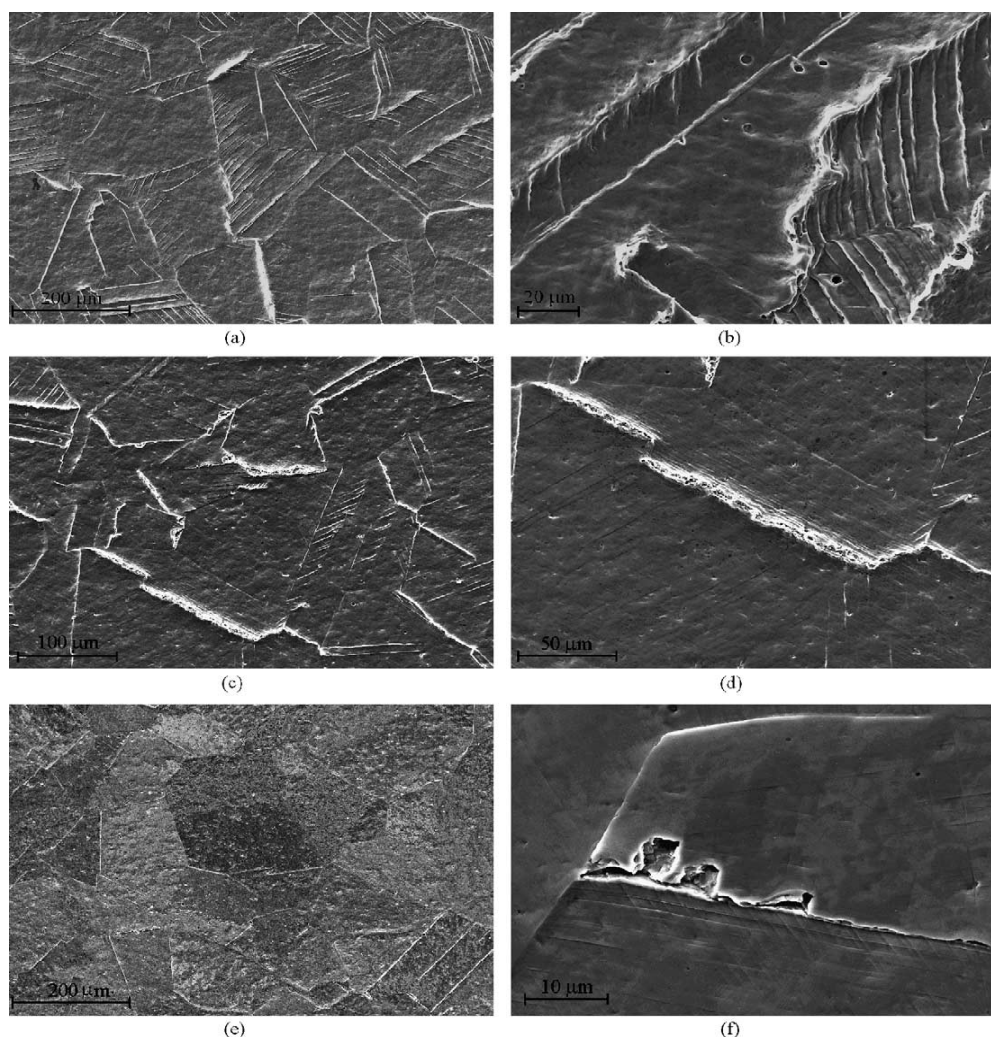


Figure 3: Surface at initial stages of CE for: (a and b) solution treated samples tested in CE after 5.4 ks, (c and d) samples with 0.33N (wt. %) at surface tested in CE after 14.4 ks and (e and f) samples with 0.48N (wt. %) at surface tested in CE after 14.4 ks.[4]

Based on the study by Jose Francisco dos Santos et. al [4], the results showed that increasing the nitrogen content in solid solution, up to 0.48 wt. %, increased the hardness. The increase in nitrogen content increases the elastic energy returned to the environment and decreases the amount of plastic energy absorbed by the alloy, at cavitations impact spots. The specimen is plastically loaded to a lesser extent and at the same time shows a greater resistance to plastic deformation due to hardening, leading to less deformed grains. As shown earlier, the mass loss inside microcavities occurs by a fatigue mechanism. The increase in nitrogen content leads to a more even deformation, to less extruded grain boundaries and to smaller amounts of microcavities. In the high nitrogen specimens, mass loss occurred mainly by microcrack formation at the first stages of damage and by a synergistic effect of microfatigue and microcrack formation at the latter stages of damage. On the other hand, in the low nitrogen specimens, mass loss occurred by microfatigue associated with microcrack formation in all stages of damage. Figure 4 below shows the hardness as a function of the nitrogen content.

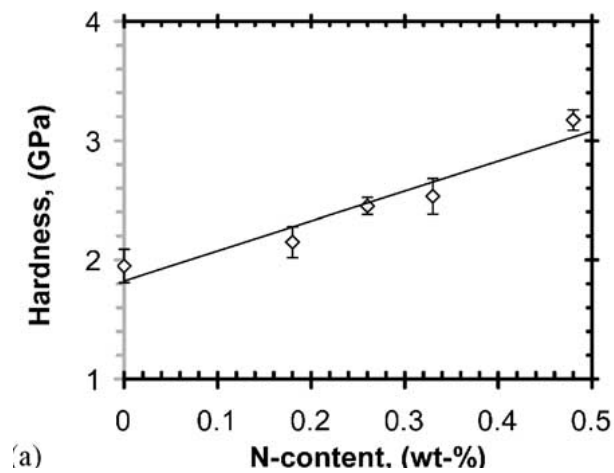


Figure 4: Hardness as a function of Nitrogen content [4]

High temperature gas nitriding treatment significantly improves the CE resistance of austenitic AISI 304L stainless steels. Increasing the nitrogen content in solid solution (up to 0.48 wt. %) through HTGN increases 4.6 times the incubation time and decreases 8.6 times the erosion rate.

2.2 Effect of partial solution nitriding on mechanical properties and corrosion resistance in a type 316L austenitic stainless steel plate.

Tomonori Nakanishi et.al [5] points out that solution nitriding had improved the properties of the austenitic stainless steel used as commercial osteosynthesis implants and to also reduce the plate thickness, type 316L austenitic stainless steel plates (AISI 316L). The solution nitriding time varied up to 36 ks to change the nitrogen concentration distribution in the steel plates, and then the material properties were investigated to demonstrate the effect of the unsaturated solution nitriding (partial solution nitriding). As a result of tensile testing for the solution-nitrided steel plates, yield strength was almost identical irrespective of the solution nitriding time even in the partially solution-nitrided specimens, while tensile strength was monotonically increased as the solution nitriding time increased and then levelled off at the maximum value when nitrogen absorption was completed. As for corrosion resistance, the solution-nitrided steel plates exhibited excellent pitting corrosion resistance even in the case of partial solution nitriding. They attempted to improve the mechanical properties and corrosion resistance of commercial 316L austenitic stainless steel plates by means of “solution nitriding” (nitrogen absorption treatment or high temperature gas nitriding (HTGN)), which is one of chemical heat treatments to add nitrogen into stainless steel. It is well known that the nitrogen addition to austenitic stainless steels has many advantages including;

- 1) The tensile strength of the steels drastically increases without reducing the ductility too much
- 2) The transformation to martensitic structures (generation of magnetism) can be reduced
- 3) Corrosion resistance, especially pitting corrosion resistance, is improved
- 4) Nitrogen is considered to be harmless to the human body.

Solution nitriding is a simple and powerful technique to obtain high nitrogen stainless steel without requiring any special equipment. In addition, the authors have also investigated the effect of solution nitriding in stainless steel thin plates where nitrogen has been fully absorbed to the state of equilibrium, resulting that the fully solution-nitrided austenitic steel has not only high strength but also large work hardening rate, thus leading to a large uniform elongation at ambient temperature. Solution nitriding is thus supposed to be one of the most effective methods to modify osteosynthesis implants through these reports.

Figure 5 below shows the optical micrographs of 316L steel solution—nitrided for 0.6ks (b) 4.8ks (c), and 36 ks (d), as well as nitrogen-free 316L steel (a). It is confirmed that the grain size of austenitic tends to be enlarged while increasing the solution nitriding time. Figure 6 displays the hardness result of the nitrided Stainless Steel. The original hardness level before solution nitriding (1.7Gpa) is also indicated by the broken line.

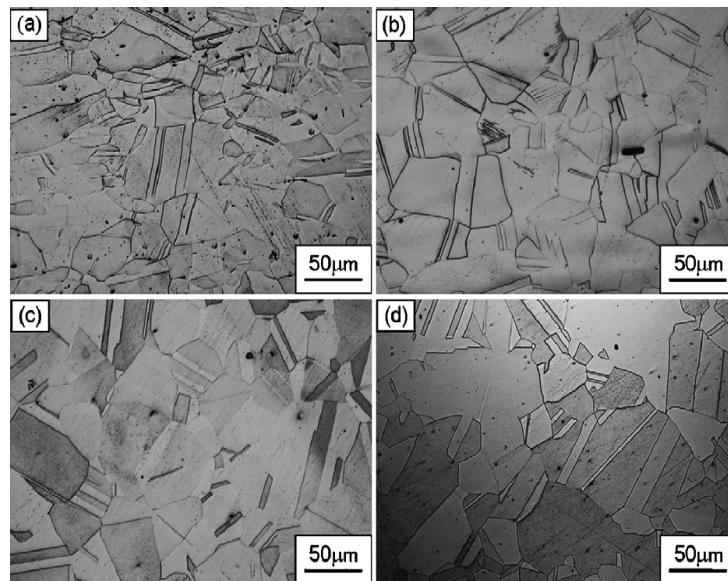


Figure 5: Optical micrographs of the nitrogen-free 316L austenitic steel (a) and solution-nitrided 316L ones (b–d). The solution nitriding was carried out at 1473 K–0.1MPa for (b) 0.6 ks, (c) 4.8 ks, and (d) 36 ks.[5]

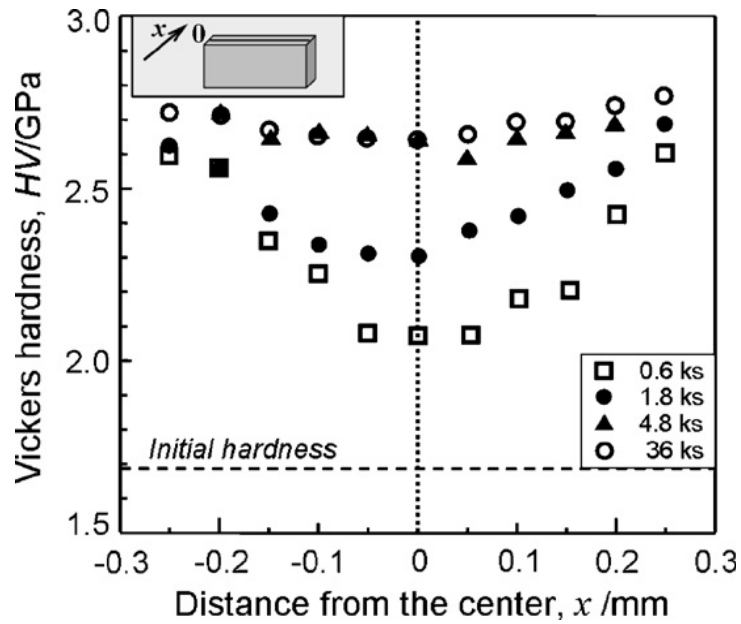


Figure 6: Vickers hardness profiles of the 316L steel solution-nitrided for 0.6, 1.8, 4.8, and 36ks. [5]

Figure 7 represents nominal stress-strain curves obtained by tensile testing for the steel A, N-0.6, N-1.8, and N-4.8. The solution-nitrided steels have much higher yield strength and tensile strength than the nitrogen-free Steel A. Figure 7 shows the changes in the yield strength and tensile strength as a function of the logarithm of the solution nitriding time. The increase in the yield strength saturates soon after starting the solution nitriding (0.6 ks), while the tensile strength was monotonically increased owing to the enlargement of work hardening rate and then it becomes constant after the system reaches the state of equilibrium (4.8 ks). The fully solution-nitrided steel, Steel N-4.8, exhibits the maximum work hardening rate and tensile strength of 900MPa. The uniform elongation was also the largest in the Steel N-4.8 among three solution-nitrided steels. The result of Figure 8 indicates that the strengthening of the surface layer with nitrogen is effective for increasing the yield strength of the whole plate specimen, which means that the long treatment time is not required in the practical viewpoint when only a high yield strength is needed for the steel plates; however, the nitrogen absorption into the core region is essential for obtaining the best performance in terms of tensile strength and uniform elongation. The fracture surface was also observed for solution-nitrided

steels to confirm their fracture mode. Figure 9 represents SEM images showing the fracture surface of Steel A and N-4.8. Both specimens exhibit typical ductile fracture though the size of dimple is slightly different between the specimens. However, no such fracture mode was observed in this study, thus suggesting the ductile-to-brittle transition temperature to be lower than the ambient temperature in the case of solution-nitrided 316L steel containing 0.46%N.

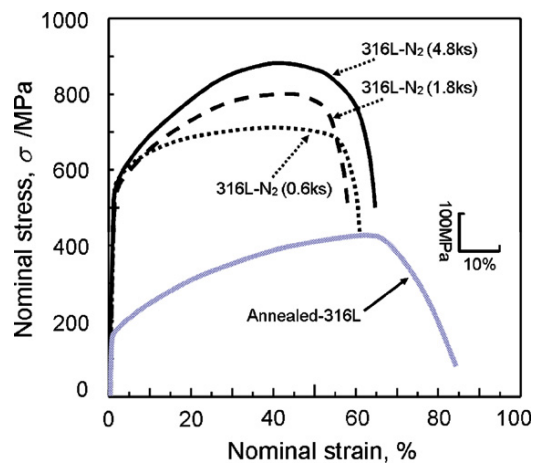


Figure 7: Nominal stress-strain curves obtained by tensile for the steel A, N-0.6, N-1.8, and N-4.8. The solution-nitrided steels have much higher yield strength than the nitrogen-free steel A.[5]

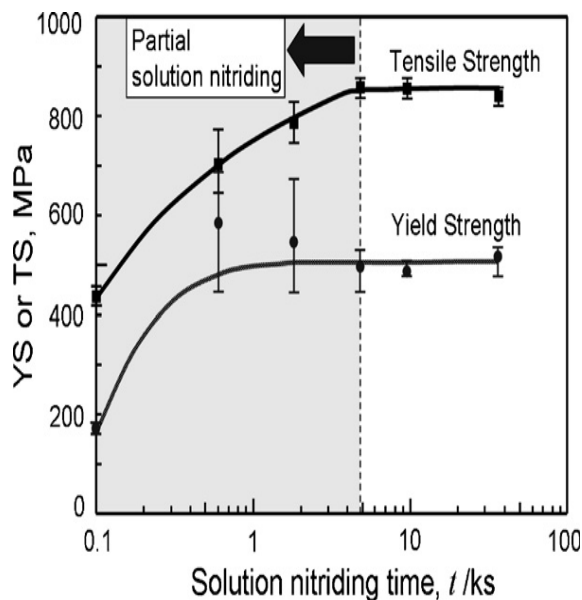


Figure 8: Changes in the yield strength and tensile strength as a function of solution

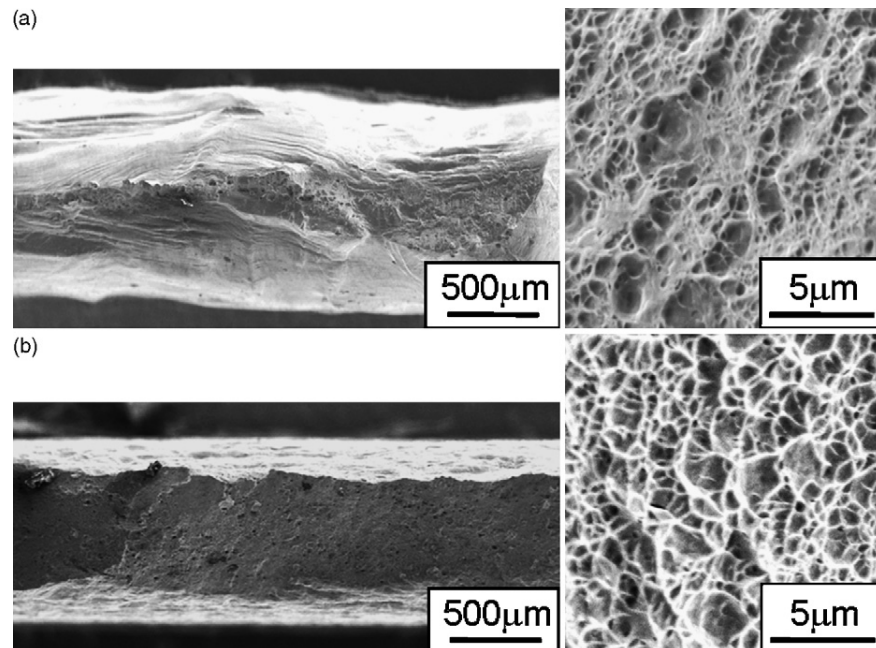


Figure 9: SEM micrographs of the fracture surfaces of plate specimens after tensile testing in (a) nitrogen-free 316L steel and (b) solution-nitrided steel (Steel N-4.8).[5]

When increasing the solution nitriding time, the yield strength rapidly increased and reached a maximum value of 550MPa before completing nitrogen absorption to the state of equilibrium. This suggests that a long treatment time is not required from a practical point of view when only high yield strength is needed for the steel plates. The tensile strength was monotonically increased with increases in the solution nitriding time and then levels off at 900MPa after the nitrogen absorption is completed. The fully solution-nitrided steel exhibits the maximum uniform elongation in spite of having a maximum tensile strength. This is due to the largest work hardening rate derived from the development of a planar dislocation structure within the whole specimen during the deformation.

2.3 Improvement of the slurry erosion resistance of an austenitic stainless steel with combinations of surface treatments: Nitriding and TiN coating.

Abel André C. Recco et.al⁴ [12] emphasize that High Temperature Gas Nitriding (HTGN) has been successfully used to improve the erosion resistance of different stainless steels. Six kinds of sample conditions were tested in a slurry composed of distilled water and SiC particles: High temperature gas nitriding (HTGN), low temperature plasma nitriding (expanded austenite), high temperature gas nitriding followed by a PVD-TiN coating, low temperature plasma nitriding followed by a PVD-TiN coating as well as PVD-TiN coated and uncoated samples in the solubilized condition. The erosion tests were performed during 6 h in a jet-like device with a normal angle of incidence and an impact velocity of 8.0 m/s. Wear rates were assessed by accumulated mass loss measurements and through analysis of scanning electron microscopy images of the worn surfaces. The results were related to the microstructure and hardness of the surface to establish a ranking of the different surface treatments. After the first few minutes of testing cutting of the surface occurred in the solubilized, in the HTGN and in the low temperature plasma nitrided AISI 304 samples, whereas TiN coated samples did not show any cutting marks, although some indentation marks could be observed. The TiN coated samples showed wear resistances one order of magnitude greater than the solubilized, HTGN and low plasma nitrided samples.[12] Solubilized (solution annealed) samples of AISI 304 stainless steel were used as base material for the different treatments. The surface of the samples was manually polished with diamond paste until 1.0 μm , washed in acetone and hot dried. The chemical analysis of the concentrations of the elements gave in wt.% Cr18.9, Ni 7.2, Mn 1.5, Mo 0.22, C 0.04, S 0.004, Fe bal. Six kinds of specimens were analyzed: solubilized, high temperature gas nitrided (HTGN), pulsed plasma nitride (expanded austenite), solubilized with a PVD-TiN layer deposition, HTGN with a PVD-TiN layer deposition and pulsed plasma nitrided plus PVD-TiN layer deposition. The solubilizing treatments were performed

with the aim of dissolving carbides present in the microstructure, and were carried out in an Ar atmosphere inside a tubular furnace described elsewhere the samples were heated up to 1373 K for 1 h and quenched in water. High temperature gas nitriding was carried out in the same equipment at 1473 K for 6 h under 0.15 Mpa N₂ pressure. After nitriding the samples were directly quenched in water. The pulsed plasma nitriding and the PVD-TiN layer deposition were carried out in a hybrid reactor. The hybrid process allows coating the pre-nitrided sample with a TiN layer without exposing the specimen to atmospheric pressure, avoiding cleaning operations of the surface between depositions. [12] The test was carried out with slurry composed by 900 ml of distilled water and 100g of angular shaped silicon carbide particles. The size of the particles was between 212 and 300 μm . The SiC abrasive particles with 26 GPa hardness are shown in figure 10. The impact angle was fixed in 90° and the velocity of the jet was 8.0 m/s. The samples were cleaned with distilled water for 10 min, dried in hot air, and weighed in a Shimadzu AUW 220D scales with a precision of 0.01 mg. Thereafter, the samples were eroded and then weighed again.[12]

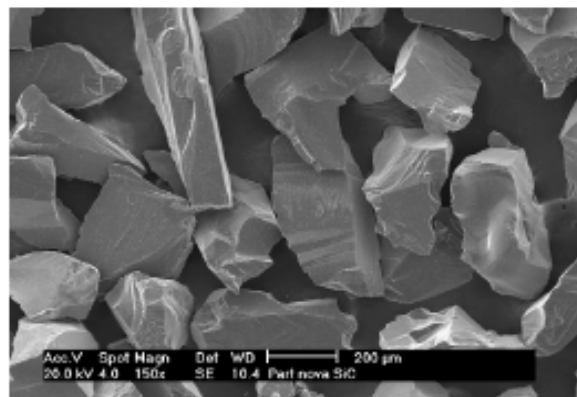


Figure 10: Morphology of Sic particles used in slurry test. [12]

Hardness values (H) measured on top of the samples for the six different conditions are shown in Table 1, together with the Young Modules (E) values and the H_{SiC}/H_{surface} ratios.

Table 1: Hardness, elastic modulus and $H_{SiC}/H_{Surface}$ ratios of the studied samples. [12]

Material	Elastic Module (Gpa)	Hardness (Gpa)	$H_{SiC}/ H_{surface}$
Solubilized	200±10.0	1.85±0.21	14.0
HTGN	200±10.0	3.17±0.35	8.2
Expanded Austenite	200±10.0	15.0±0.9	1.7
Solubilized + Tin	430±25.6	21.86±2.14	1.2
Expanded austenite + Tin	425±23.4	22.50±1.81	1.2
HTGN + TiN	435±19.5	21.54±2.21	1.2

Accumulated mass losses as a function of time are presented in Figure 11 for the six surface treatment conditions. The calculated wear rates are shown in the Table 2. They are calculated through the slopes of the mass loss curves shown in Figure 11.

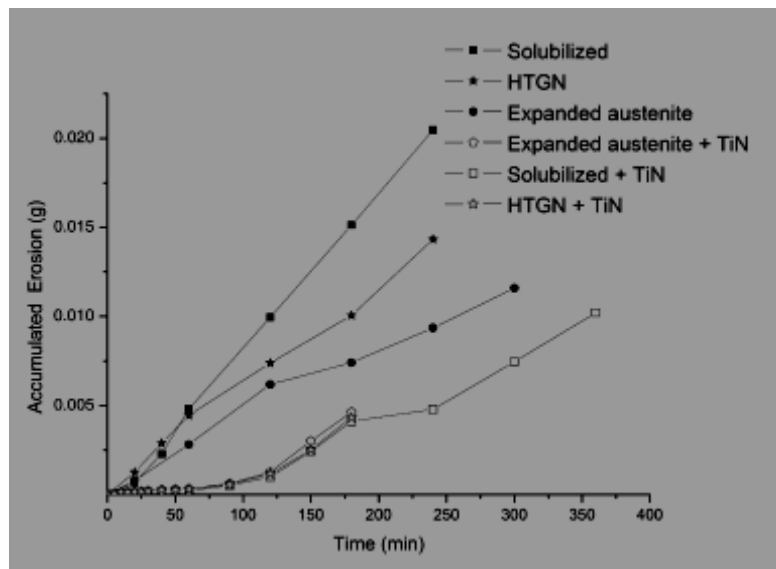


Figure 11: Accumulated erosion as a function of exposure time. [12]

Table 2 : Erosion rates of the specimens. [12]

Sample	Erosion rate ($\mu\text{g}/\text{min}$)	Interval of time (min)	Correlation coefficient, R
Solubilized	88.0	240.0	0.999
HTGN	57.0	240.0	0.996
Expanded austenite	43.0	240.0	0.992
Solubilized + TiN	4.3	60.0	0.961
HTGN + TiN	4.8	60.0	0.956
Expanded austenite + Tin	5.2	60.0	0.975

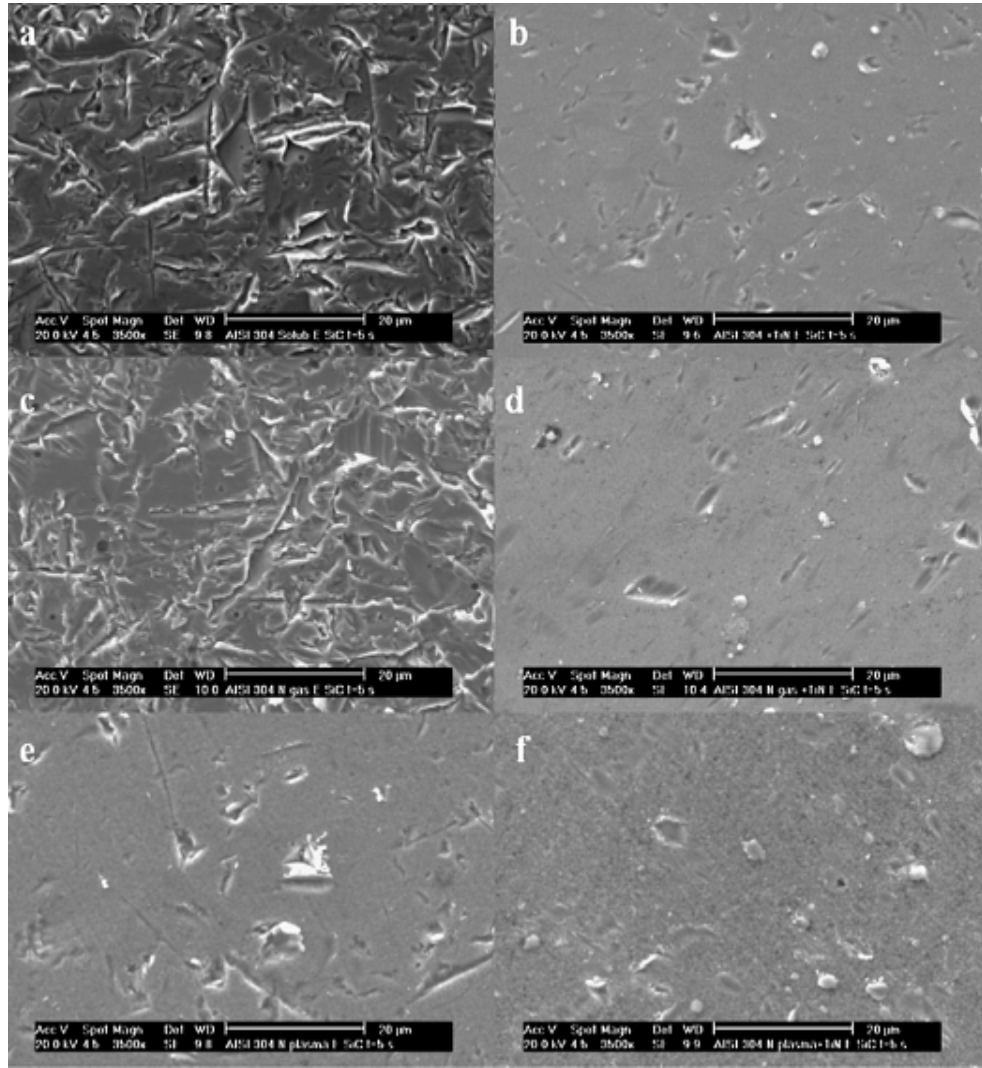


Figure 12 : SEM of the surface of the samples after 5 seconds testing: a) Solubilized, b) Solubilized+TiN, c) HTGN, d) HTGN+TiN, e) Expanded austenite and f) Expanded austenite + TiN.[12]

Figure 12 show the scanning electron micrographs of the worn surfaces at the first seconds of testing and after one hour testing, respectively. The solubilized specimen shows considerable amounts of cutting marks since the beginning of the test. The worn surface reveals lips and craters and allows observing the way the particles cut the surface. A similar topography is observed for the HTGN sample (Fig. 12a and c). The surface of the plasma nitrided specimen is shown in Fig. 12e. The number of cutting marks decreases and some indentation marks can be observed. The samples coated with the TiN layer showed a considerably reduced number of cutting and indentation marks on the surface (Fig. 12 b, d and f). The mass removal

mechanism observed in the solubilized and HTGN samples was cutting, in spite of the normal incidence of the particles.[12]

After testing an AISI 304 austenitic stainless steel submitted to high temperature gas nitrided, low temperature pulsed plasma nitriding, and PVD-TiN coating, in slurry made of water containing SiC particles, it is possible to conclude [12]:

1. High temperature gas nitriding reduced 1.5 times the wear rate of the austenitic stainless steel.
2. Low temperature pulsed plasma nitriding reduced 2 times the wear rate of the austenitic stainless steel.
3. PVD-TiN coatings deposited over different surface treatments of the austenitic stainless steel reduced the wear rate by 20 times.
4. The mechanical properties of the substrate did not affect the erosion rate of the TiN coated specimens.
5. When the TiN coating is removed, the effect of the substrate hardness differences is observed and intense cutting of the samples is observed.

CHAPTER 3

METHODOLOGY

3.1 Nitriding Experiment

The experiment started with 1 hour nitriding time which is known as preliminary experiment before proceeding with longer period of diffusion. Several tests needed to be carried out after the nitriding process was performed. The experiment was conducted successfully and all the testing were achieved effectively. The samples show the arrangement in the Alumina boat (see Figure 13). The boat was then pushed by a long stick to ensure the samples were placed in the middle of the furnace (see Figure 14). Every step was needed to be followed properly and personal protection equipment must be worn while performing the experiment.



Figure 13: Sample arrangement in the Alumina Boat



Figure 14: Alumina boat was pushed into the tube furnace

The procedure of the Nitriding experiment is as follow;

At the beginning;

1. The cover of the tube furnace was opened.
2. The sample was pushed into the middle of tube furnace
3. The furnace cover was closed.
4. Air was purged in the furnace for about 15 minutes.
5. The instruction on the controller was set and followed.

Nitrogen Flow

1. Argon gas valve was closed.
2. Outlet flow argon was closed.
3. Gas inlet pipe was changed to N₂
4. The N₂ gas valve was opened.
5. Pressure inlet of N₂ gas was set at 14.5psi
6. Flow meter (rate) at 3 scale was set.

Quenching

1. N₂ gas Valve was close.
2. N₂ inlet valve was close.
3. The cover of tube furnace was opened
4. The insulation plug was take out from the tube furnace
5. The sample was pulled out from heating zone in a short period.
6. The sample was took out and quench it into the water at room temperature.

End

1. Switch off power (furnace)
2. Check all the gas valve (closed position)

3.2 Metallographic

Metallography is the science and art of preparing a metal surface for analysis by grinding, polishing, and etching to reveal microstructural constituents. After preparation, the sample can easily be analyzed using optical or electron microscopy.

3.2.1 Sectioning

After the samples were received, they were cut into required sizes. The objective is to prepare for tests other than microstructure or macrostructure structure. The tool that author used to cut the specimen is abrasive cutter. Abrasive cutting is the sectioning of material using a relatively thin rotating disk composed of abrasive particles supported by a suitable medium. Figure 15 show the abrasive cutter used to cut the sample. Each sample was cut to same size which is 60mm (see Figure 16).



Figure 15: Abrasive Cutter



Figure 16: 316L Stainless Steel sample

3.2.2 Mounting

Metallographic specimens were cut to an appropriate size, mounting of the specimen is often desirable or necessary for subsequent handling and metallographic polishing. The specimen was placed in the mounting press, the resin was added, and the sample was processed under heat and high pressure (see Figure 17). The pressure used to mount the resin was set to 1200psi. Time allocated for the heat time was about one minute and for the cooling time was about 5 minutes. The machine used to mount the sample is Simplimet Auto Mounting Press (see Figure 18).



Figure 17: Hot Mounting



Figure 18: Simplot Auto Mounting Press

3.2.3 Grinding

Investigations continue by grinding the mounted specimen to the parallel surface finish. The abrasive particles are forced into a flat surface of a comparatively soft material. The specimen is successively ground with finer and finer abrasive media. Silicon carbide sandpaper was the first method of grinding and is still used today. Many metallographers, however, prefer to use a diamond grit suspension which is dosed onto a reusable fabric pad throughout the polishing process. Diamond grit in suspension might start at 9 micrometers and finish at one micrometer. Generally, polishing with diamond suspension gives finer results than using silicon carbide papers (SiC papers), especially with revealing porosity, which silicon carbide paper sometimes "smear" over. Because the austenitic grades work harden readily, cutting and grinding must be carefully executed to minimize deformation. The machine used to grind the sample s METASERV 1000 (see Figure 19).



Figure 19: METASERV 1000 grinder and polisher machine

3.2.4 Polishing

After grinding the specimen, polishing was performed. Typically, a specimen was polished with slurry of alumina, silica, or diamond on a napless cloth to produce a scratch-free mirror finish, free from smear, drag, or pull-outs and with minimal deformation remaining from the preparation process.

3.2.5 Etching

After polishing the sample, microstructural constituents of the specimen were revealed by using a suitable chemical or electrolytic etchant. A great many etchants have been developed to reveal the structure of metals and alloys, ceramics, carbides, nitrides, and so forth. While a number of etchants may work for a given metal or alloy, they generally produce different results, in that some etchants may reveal the general structure, while others may be selective to certain phases or constituents. The etchants that author used for the austenitic stainless steel are Glyceregia. Author had chosen the best etchant which is Glyceregia's reagent, the ingredient for this particular etchant are;

- a) 45ml Glycerol.
- b) 15ml Nitric Acid
- c) 30ml Hydrochloric Acid

The procedure of etching;

- a) Specimen was cleaned by the distilled water.
- b) Next, specimen was dip with the alcohol to remove the dirt and contamination.
- c) Then, the specimen was pour with a little etchant (Glyceregia's Reagent).
- d) After 10minutes the specimen was rinsed with distilled water.
- e) Again, the specimen was dip in the Alcohol.
- f) Finally, the specimen was dried by using the dryer.

3.2.6 Light Microscopy

Light optical microscopy remains the most important tool for the study of microstructure. At first the magnification start with low magnification, such as 5x, followed by progressively higher magnification for efficient assessment of the basic characteristic of the microstructure.

3.3 Vickers Hardness Testing

Vickers Hardness tester was used to measure the hardness of the sample. The basic principle, as with all common measures of hardness, is to observe the questioned materials' ability to resist plastic deformation from a standard source. The Vickers Hardness test can be used for all metals and has one of the widest scales among hardness tests. The maximum load applied is 300g. The machine that author used to perform the hardness test was micro hardness tester Model LECO LM247 AT. Figure 20 below shows the indentation process by using Vickers hardness.



Figure 20: Indentation process by using Vicker Hardness

3.4 Tensile Test

After the hardness and microstructure analysis were done, tensile test was used to measure the maximum tensile strength for the as received sample, 1 hour and 5 hours diffusion. This test is very important to see how the material reacts to forces being applied in tension. The sample was gripped at either end by suitable apparatus in a testing machine which slowly exerts an axial pull so that the steel is stretched until it breaks by using UTM 100kN (see Figure 21). The test provides information on proof stress, yield point, tensile strength, elongation and reduction of area. According to the standard, there were 3 samples being test and the size of the sample is determined by the E8M Standard (see Figure 22 and Table 3).

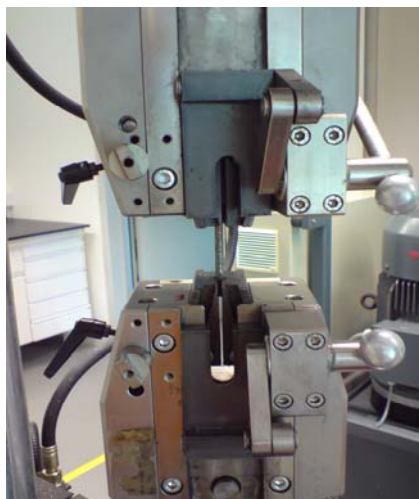


Figure 21: UTM 100KN

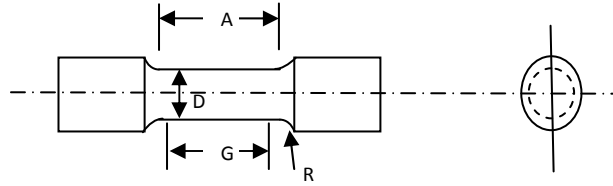


Figure 22: Schematic drawing for metal rod

Table 3: Standard dimension for tensile test E8M

Dimensions, mm					
	Standard Specimen		Small-size Specimens Proportional to Standard		
	12.5	9	6	4	2.5
G- Gage Length	62.5±0.1	45.0±0.1	30.0±0.1	20.0±0.1	12.5±0.1
D-Diameter (Note 1)	12.5±0.2	9.0±0.1	6.0±0.1	4.0±0.1	2.5±0.1
R- Radius of Fillet. Min	10	8	6	4	2
A-Length of Reduced section,min	75	54	36	24	20

Source: ASTM Standards E8M , “ Standard test Methods for tension Testing of Metallic Materials

CHAPTER 4

RESULT AND DISCUSSION

4.1 Metallographic Result

Figure 23 shows the optical micrographs of 316L steel solution nitrogen-free 316L steel (a) nitrated for 1 hour (b) 5 hours (c), and 9 hours (d). This experiment was done in the tube furnace where the sample was heated for 1 hour at 1200°C and purged by Nitrogen gas. By comparing the microstructure from the raw material (a) to the nitrating sample (b-d), there is no much different in size. It is predictive without changing the microstructure, the figures show that the austenitic structure remains the same. There is an indication but it is not obvious. In addition, the sizes of the microstructure slightly increase by extending the nitrating time from 1 hour to 9 hours. The twin structure is the austenitic structure and it remains the same while changing the nitrating time. The slip band was produced during the manufacturing of the metal rod and it was then removed by performing the normalizing experiment. Normalizing is the annealing process used to refine the grains, and produce a more uniform and desirable size distribution [11].

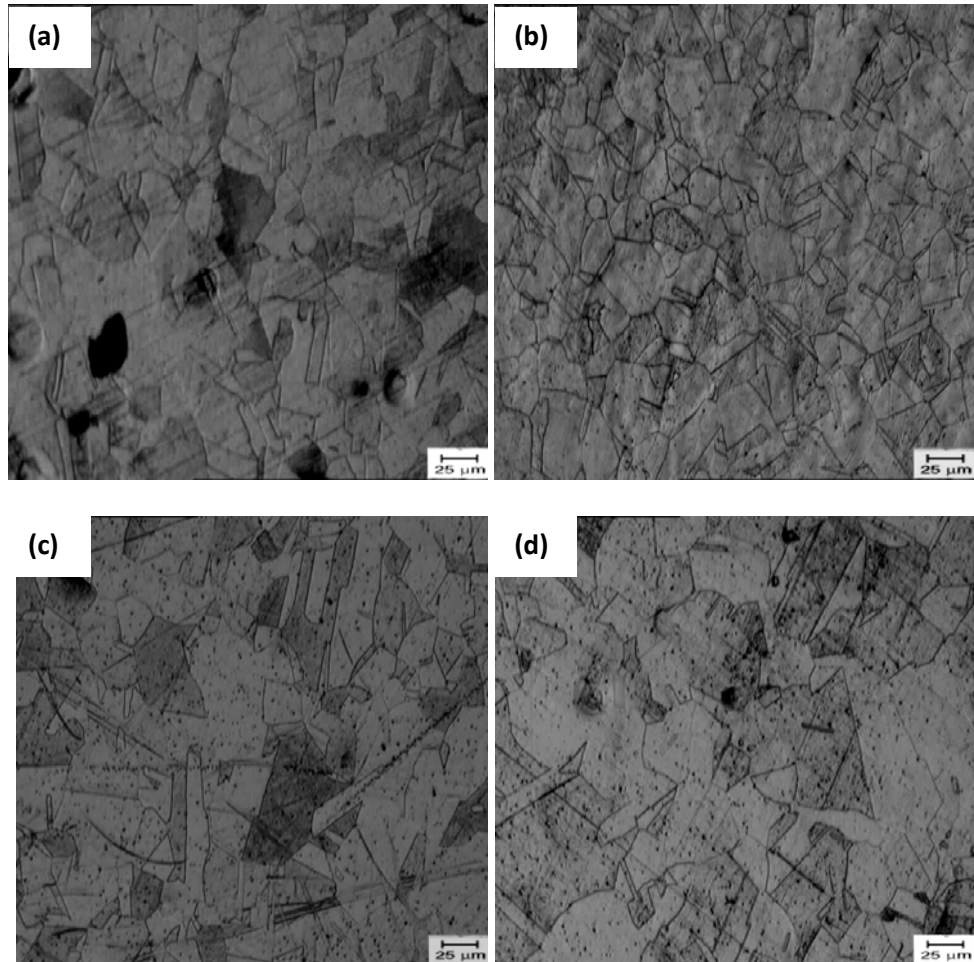


Figure 23: Microstructure of (a) Normalizing sample Mag(50x) ,(b) 1hour(50x) , (c) 5 hours Mag(50x),(d) 9 hours Mag(50x) nitriding time at 1200°C of 316SS.

4.2 Vickers Hardness result

Based on the experiment of determining the hardness of the as received sample, 1 hour, 5 hours and 9 hours nitriding time, it was found that the highest hardness value is 430Hv for 9 hours nitriding time. The percentage of increase for the normalizing to 9 hours sample is 130%. Experimentally, the longer time of nitriding time significantly produces higher hardness value. According to this graph, the distance variable influences the hardness result which is show by fluctuate result during the test (see Figure 24). The lowest value of hardness is located at the core of the austenitic stainless steel sample. This is because of the diffusion capabilities of nitrogen into the surface of the sample. There is a certain depth for the nitrogen adsorption into the structure depends on the nitriding time.

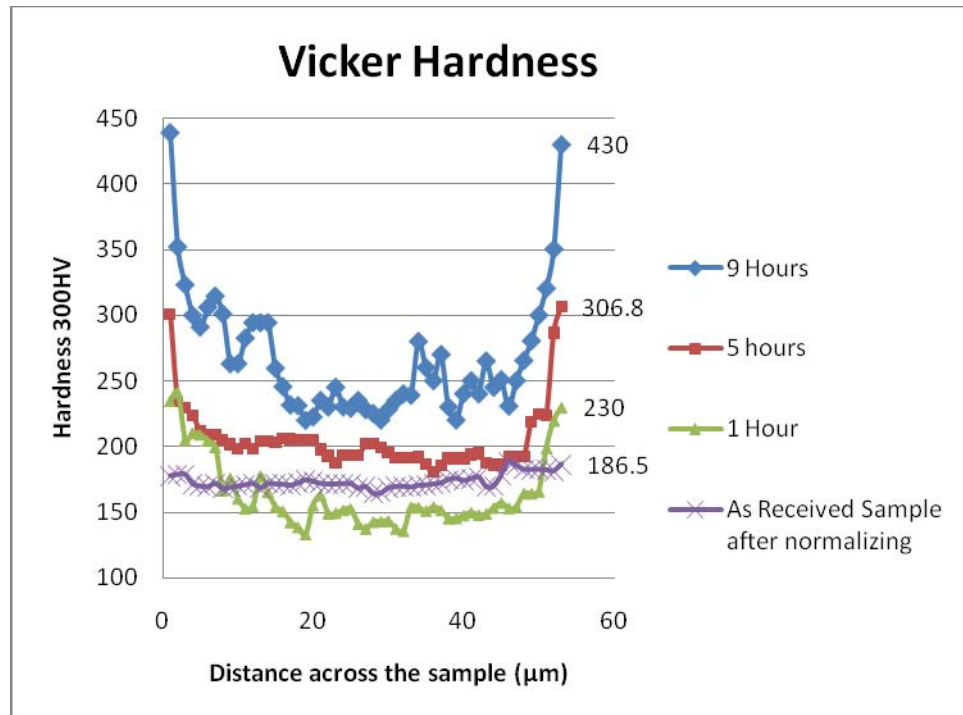


Figure 24: Hardness value of as received sample, 1 hour, 5 hours and 9 hours diffusion of Nitrogen into Austenitic Stainless Steel

4.3 Tensile test result

Figure 25 shows the stress strain curve for the overall sample from the as received sample until 9 hours nitriding time. The value of the ultimate tensile stress (UTS) for the as received sample is 524.16N/mm^2 , 1 hour nitriding time is 538.64N/mm^2 , 5 hours is 556.88N/mm^2 and the highest ultimate tensile strength is 559.23N/mm^2 for the 9 hours (see Table 4). A small constriction or neck begins to form at some point from 500 to 550N/mm^2 , and all subsequent deformation is confined at this neck. The UTS significantly increases when the diffusion time increased. This phenomenon is termed “necking”, and fracture ultimately occurs at the neck (see Figure 26). Ordinarily, when the strength of a metal is cited for design purposes, the yield strength is used. Ductility is another important mechanical property. From the result, the ductility value for the as received sample slightly less than the nitride sample. It proves that the nitriding experiment had affected the ductility of the respective sample. Ductility is measure of the degree of plastic deformation that has been sustained at

fracture [11]. Yield strength is also important which is the stress corresponding to the intersection of this line and the stress- strain curve as it bends over in the plastic region. In order to determine the yield strength, a straight line is constructed parallel to the elastic portion of the stress strain curve at some specified strain offset, usually 0.002. Based on the experiment, the yield strength of the nitrided sample gave higher value compared to the as received sample.

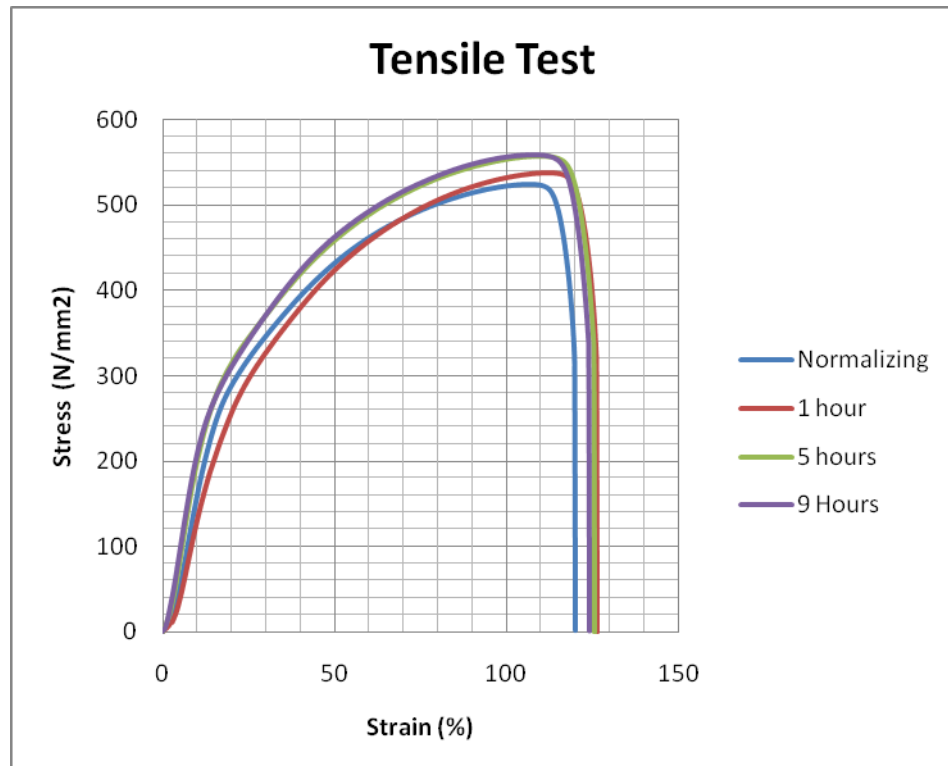


Figure 25: Stress Strain curve for normalizing, 1 hour, 5 hours, 9 hours of Nitrogen diffusion on austenitic Stainless Steel



Figure 26: Necking portion of the testing sample

Table 4 : Summary of stress strain curve

	Ultimate Tensile Strength (MPa)	Yield Strength (MPa)	Ductility (%)
Normalizing	524.16	220	119.5
1 Hour	538.64	210	126.43
5 Hours	556.88	230	125.66
9 Hours	559.23	235	124.11

CHAPTER 5

CONCLUSION

Type 316L type austenitic stainless steel rod (AISI 316L) were subjected to gas nitriding for various time of diffusion at constant temperature of 1200^oC, and the effect of gas nitriding time on the mechanical properties and physical properties were investigated. The results obtained are summarizes as follow:

- a) The nitriding had improved the mechanical properties of the raw material. Increasing the nitriding time trough high temperature gas nitriding increases 130% hardness from the normalizing to the 9 hour diffusion time.
- b) The ultimate tensile strength (UTS) and ductility significantly increases when the diffusion time increased. The highest UTS collected during experiment was 559.23Mpa from 9-hours diffusion.
- c) The microstructures of the raw material remain the same when nitriding is performed. This is due to the crystalline structure of the austenitic which is face centered cubic (FCC). The nitriding may not be able to expand the bond between molecules on the FCC structure. But for the nitriding sample gave different result, it was shown that the microstructure slightly expands but it is not obvious and significant.
- d) The mechanical properties of hardness and tensile strength had significantly increased the austenitic AISI 316L stainless steels samples by performing Nitriding experiment.

REFERENCES

- [1]. Donald R. Askeland, *The Science and Engineering of Materials*, Thomson.
- [2]. info@metalinfo.com, 2002, <<http://metals.about.com/bldef-Alloying-Element.htm>>
- [3]. *ASM Metals Handbook volume 9, metallography and microstructure 2004*. ASM International.
- [4]. Carlos Mario Garzon, Andre Paulo Tschitschin, *Improvement of the cavitation erosion resistance of an AISI 304L austenitic stainless steel by high temperature gas nitriding*, 2004.
- [5]. Toshihiro Tsuchiyama, Hiromichi Mitsuyasu, Yukihide Iwamoto, Setsuo Takaki, *Effect of partial solution nitriding on mechanical properties and corrosion resistance in a type 316L austenitic stainless steel plate*, 2007
- [6]. George E. Totten, *Steel Heat Treatment, Metallurgy and Technologies*, CRC Press; Taylor Francis Group.
- [7]. Fontana, M.G., *Corrosion Engineering*, 3rd Ed, McGraw-Hill, New York, 1987
- [8]. J.R Davis, *Surface Hardening of Steels, Understanding the Basics*, ASM International; The Materials Information Society.
- [9]. Romesh C. Sharma, *Principle of Heat Treatment of Steels*, New Age International Publisher, 2003.
- [10]. H.S Khatak, *Corrosion of Austenitic Stainless Steels, mechanism, mitigation and monitoring* 2002, WoodHead Publishing Limited.

- [11]. William D. Callister, Jr. David G. Rethwisch , Fundamental of Material Science and Engineering 3rd Edition, John Wiley & Sons, Inc.
- [12]. Abel André C. Recco, Diana López, André F. Bevilacqua, Felipe da Silva, André P. Tschiptschin, Improvement of the slurry erosion resistance of an austenitic stainless steel with combinations of surface treatments: Nitriding and TiN coating, 2007